

Photoluminescence study of disordering in the cation sublattice of $\text{Cu}_2\text{ZnSnS}_4$



M. Grossberg*, J. Krustok, T. Raadik, M. Kauk-Kuusik, J. Raudoja

Tallinn University of Technology, Ehitajate tee 5, 19086 Tallinn, Estonia

ARTICLE INFO

Article history:

Received 26 June 2014

Received in revised form

31 July 2014

Accepted 18 August 2014

Available online 27 August 2014

Keywords:

Kesterite

$\text{Cu}_2\text{ZnSnS}_4$

Photoluminescence

Defects

ABSTRACT

In this study we investigated the influence of the degree of disordering in the cation sublattice on low temperature photoluminescence (PL) properties of $\text{Cu}_2\text{ZnSnS}_4$ (CZTS) polycrystals. The degree of disordering was changed by using different cooling rates after post-annealing at elevated temperatures. The results suggest that in the case of higher degree of cation sublattice disorder radiative recombination involving defect clusters dominates at $T = 10$ K. These defect clusters induce local band gap energy decrease in CZTS. The concentration of defect clusters can be reduced by giving more time for establishing ordering in the crystal lattice. As a result, radiative recombination mechanism changes and band-to-impurity recombination involving deep acceptor defect with ionization energy of about 200 meV starts to dominate in the low temperature PL spectra of CZTS polycrystals.

© 2014 Published by Elsevier B.V.

1. Introduction

$\text{Cu}_2\text{ZnSnS}_4$ (CZTS) is estimated as relatively cheap indium-free absorber material for thin-film solar cells. In 2013, an IBM group reported 12.6% efficiency of a $\text{Cu}_2\text{ZnSn}(\text{S},\text{Se})_4$ (CZTSSe) solar cell by hydrazine-based solution processing [1]. However, the record efficiency of similar CuInGaSe_2 (CIGS)-based solar cells has reached 20.9% [2]. To improve the conversion efficiency of CZTS-based solar cells, it is important to obtain more detailed information of the fundamental physical properties on CZTS material itself. Especially important is the defect structure of this material. Several theoretical calculations have shown extremely low formation energies of different defect clusters in CZTS [3,4]. These defect clusters will either produce deep recombination centres for electron–hole pairs or cause trapping of charge carriers. Both mechanisms are detrimental to solar cell parameters and should be avoided. Additionally, high concentration of intrinsic defects in CZTS leads to the formation of spatial potential fluctuations and to a local perturbation of the band structure. Some of these defects are related to the structural disorder in the cation sublattice of the host lattice. The general consensus is that the kesterite structure (space group $I\bar{4}$) is the ground-state structure in CZTS, but according to the theoretical calculations [3] the difference in the binding energy of different

polytypes is only on the order of few meV per atom. This indicates that the disorder in the cation sublattice and especially between Cu and Zn may occur under standard growth conditions. The disorder is predicted to cause bandgap energy difference of around 0.1 eV for the kesterite and the disordered kesterite structure in CZTS, the kesterite having the largest bandgap energy [3]. Neutron diffraction measurements [5,6] also showed that a partially disordered kesterite structure with an effective $I\bar{4}2m$ space group exists and the degree of disorder depends on cooling rate after sample synthesis. Rapid cooling usually gives the highest degree of disorder, while slow cooling at a rate of 1 K/h tends to give more ordered CZTS samples [5,6]. This fact was recently confirmed by near-resonant Raman scattering measurements, where the low temperature ($T \approx 533$ K) transition between ordered and disordered CZTS was discovered [7]. According to this study, the ordered CZTS is only possible below this temperature, although finite amount of disorder is expected to be present for $T > 0$ K. Low temperature ($T < 600$ K) phase transitions in quite similar $\text{Cu}_2\text{ZnGe}(\text{Se}_{1-x}\text{S}_x)_4$ compounds were also discovered in Ref. [8]. It should be mentioned that experimentally it is quite difficult to distinguish between ordered and disordered CZTS, because both structures have very similar Raman and X-ray diffraction spectra. Recently, the coexistence of ordered and disordered kesterite phases was proved using photoluminescence (PL) and Raman scattering measurements in high-quality polycrystalline CZTS [9].

It is known that the low temperature PL spectrum of CZTS usually consist of single asymmetric peak at about 1.3 eV [10–13].

* Corresponding author. Tel.: +372 620 3210.

E-mail addresses: mgross@staff.ttu.ee, maarja.grossberg@ttu.ee (M. Grossberg).

Several research groups have shown that CZTS samples have properties of highly compensated and heavily doped semiconductors with fluctuating potentials [12–14]. According to theory, the luminescence spectrum from a semiconductor with fluctuating potentials is usually dominated by three recombination channels: band-to-impurity (BI), band-to-tail (BT), and band-to-band (BB) [15,16]. BT and BI bands usually dominate at low temperatures and the peak position of both bands can be found as $h\nu_{\max} = E_g - E_T$, where E_g is a bandgap energy and E_T is a thermal quenching activation energy. However, the thermal quenching activation energy of this low temperature PL band in CZTS shows quite different values and therefore different recombination channels are expected. For example, our low-temperature PL measurements of near-stoichiometric CZTS monograins and polycrystals revealed a recombination between electrons and holes in the quantum well caused by the $(2\text{Cu}_{\bar{z}_n} + \text{Sn}_{\bar{z}_n}^2)$ defect clusters that induce a significant local band gap decrease of 0.35 eV in CZTS [11]. This kind of recombination with PL peak at $h\nu \approx 1.3$ eV differs from BT and BI recombination and seems to be a dominant one in majority of cases. It is characterized by a relatively low ($E_T < 100$ meV) thermal quenching activation energy. It is obvious, that disordered CZTS with very high concentration of defects in the cation sublattice is needed for this type of recombination.

Another PL process was detected in CZTS involving BI recombination (also with $h\nu_{\max}$ at about 1.3 eV) with very high ($E_T = 280$ meV) thermal quenching activation energy [9]. This recombination is probably not related to defect clusters and is an indication of relatively low degree of disordered phase in CZTS. Thus, the PL spectroscopy seems to be very sensitive method for defect studies in CZTS. In this study we used Raman spectroscopy and low temperature PL spectroscopy for following the disorder in CZTS polycrystals annealed at elevated temperatures and cooled to room temperature with different cooling rate.

2. Experimental details

Polycrystalline CZTS powder was prepared by solid state reaction of elemental metal powders and chalcogen in proportions corresponding to the composition of the $\text{Cu}_{1.85}\text{Zn}_{1.1}\text{Sn}_{1.0}\text{S}_{4.124}$ compound. The mixture was ground in an agate mortar. The milled powder was placed in quartz ampoules which were sealed under vacuum. For the synthesis, the temperature of the furnace was increased from room temperature to 773 K with a rate of 1.6 K/min. Then, the temperature was increased with a rate of 6 K/min up to 1123 K. A complete homogenization was obtained by keeping the mixture at 1123 K for 24 h. After that, the temperature was lowered to 573 K with a slow rate 0.15 K/min and the furnace was switched off until the tube reached room temperature. Then, the ampoule was removed from the furnace and was broken to obtain the synthesized ingot. The synthesized powder was divided into small quartz ampoules, heated to 873 K and then cooled down with different cooling rate.

For PL measurements, the powder crystals were removed from the quartz ampoule and mounted in the closed-cycle He cryostat and cooled down to 10 K. The PL measurements were performed to the fresh samples taken from the quartz ampoules after the heat treatment and also to the so-called aged samples that were exposed to air for weeks. However, no difference in the PL results of fresh and aged samples could be detected. The 441 nm He–Cd laser line was used for PL excitation and the spectra were detected by using InGaAs detector. For the phase analysis of the samples the room temperature Raman spectra were recorded by using the Horiba's LabRam HR800 spectrometer equipped with a multichannel CCD detection system in the backscattering configuration using 633 nm laser line.

3. Results and discussion

According to Scragg et al. [7], the ordering of Cu and Zn atoms in the cation sublattice can begin at temperatures below the order-to-disorder transition temperature at 533 K. Accordingly, the degree of disorder is determined by the cooling rate at temperatures below 533 K. In this study we used 6 different cooling rates in the temperature region from 573 K to 473 K: 840 K/min, 180 K/min, 24 K/min, 7.5 K/min, 0.3 K/min and 0.001 K/min. The latter cooling rate 0.001 K/min resembles low-temperature heat-treatment where the powder was kept at $T = 473$ K for a week. Typical Raman spectrum of CZTS polycrystalline powder measured with 633 nm laser excitation is shown in Fig. 1. Broadening of the A_1 Raman peak at 339 cm^{-1} was detected with increasing cooling rate (see inset graph in Fig. 1) indicating increasing degree of disorder. It has been shown [9] that the A_1 Raman peak that is often found to be asymmetric, consists of two peaks – the dominating A_1 peak of the kesterite and a shoulder peak at lower wavenumber side at about 334 cm^{-1} corresponding to the disordered kesterite. However, these two peaks are often not resolved and the degree of disorder can be estimated by using the full width at the half maximum (FWHM) of the A_1 peak, as was also shown in Ref. [7]. Moreover, it was proposed that the intensity ratio of the A_2 and A_3 Raman modes at 288 cm^{-1} and 304 cm^{-1} , respectively, can be used to estimate the degree of disorder [7], however in the present study such correlation was not detected.

On the inset graph of Fig. 1 two regions can be distinguished: the FWHM of the A_1 peak is larger for the samples with cooling rate above 24 K/min indicating higher degree of disorder, and lower values of FWHM of A_1 peak were determined for the samples with cooling rate below 10 K/min indicating more ordered material.

The low temperature photoluminescence spectra of CZTS polycrystals with different cooling rate are presented in Fig. 2. All PL spectra consist of one broad asymmetric PL band that shifts towards lower energies with increasing cooling rate (see inset graph in Fig. 2) except for the lowest cooling rate that shifts the PL band back to lower energies. Also, slight broadening of the PL band with increasing cooling rate was observed. From the slope of the low energy side of the PL band, the average depth of the potential fluctuations was determined [15] and was found to be approximately the same (about 22 meV) for all studied CZTS polycrystalline powders with different cooling rates. This implies that the overall defect concentration is not changed.

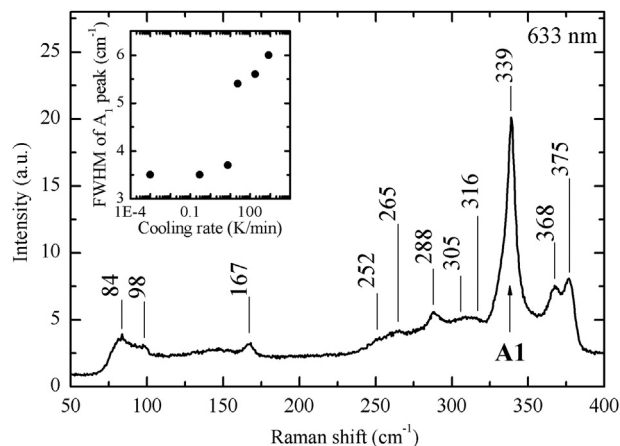


Fig. 1. Typical Raman spectrum of CZTS polycrystals measured by using 633 nm laser for excitation. The dependence of the FWHM of A_1 Raman peak on cooling rate is shown on the inset graph.

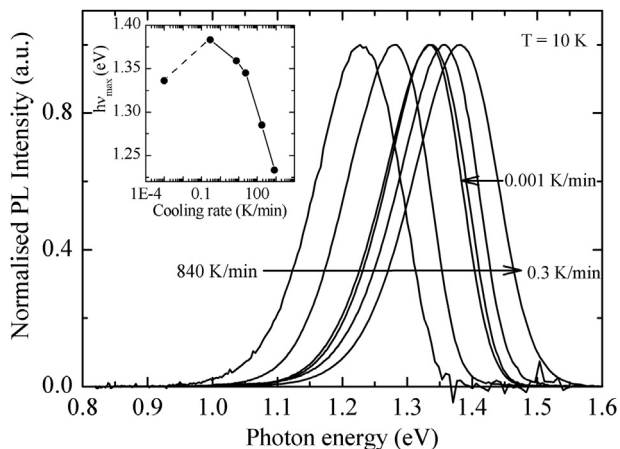


Fig. 2. Low temperature PL spectra of CZTS polycrystals with different cooling rate. The inset graph shows the dependence of the PL band maxima on the cooling rate.

As mentioned in the introduction, BT and BI bands usually dominate at low temperatures in semiconductors with high defect concentrations and the peak position of both bands can be found as $h\nu_{\max} = E_g - E_T$, where E_g is a bandgap energy and E_T is a thermal quenching activation energy. The thermal activation energies E_T were determined from the temperature dependencies of the PL spectra (see Fig. 3 and Fig. 4). For the CZTS polycrystals with cooling rate above 7.5 K/min, E_T values around 100 meV were found. For the two low cooling rates 0.3 K/min and 0.001 K/min, E_T values around 200 meV were determined. The inset graph in Fig. 4 presents the sum of E_T and $h\nu_{\max}$ in dependence of the cooling rate. It can be seen that for the two lowest cooling rates the sum of E_T and $h\nu_{\max}$ adds up to about 1.6 eV that corresponds to the low temperature bandgap energy value of kesterite CZTS [14]. This implies that for the two lowest cooling rates, BI-recombination involving relatively deep acceptor level with ionisation energy around 200 meV is dominating. On the other hand, for the higher cooling rates above 7.5 K/min, the formula $h\nu_{\max} = E_g - E_T$ is not valid anymore.

In our previous study [11], we have shown that recombination between electrons and holes in the quantum well, caused by the defect clusters that induce a significant local band gap decrease of 0.35 eV in CZTS, is characterized by a relatively low ($E_T < 100$ meV) thermal quenching activation energy. Due to the local band gap decrease, the sum of E_T and $h\nu_{\max}$ does not add up to the bandgap energy value of CZTS. Thus, recombination involving defect clusters seems to be dominating at low temperatures in CZTS with

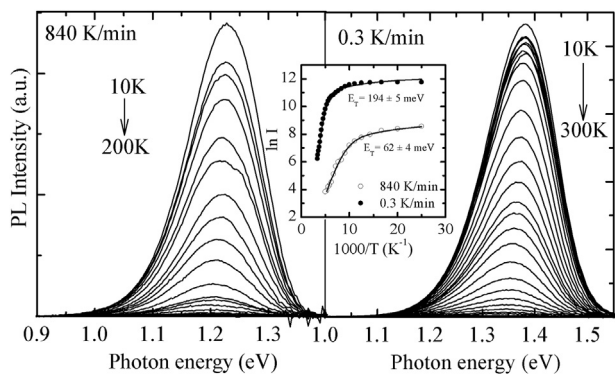


Fig. 3. The temperatures dependencies of the PL spectra for samples with cooling rates 840 K/min and 0.3 K/min together with the corresponding Arrhenius plot, where the thermal quenching activation energies were determined by using theoretical expression presented in [17].

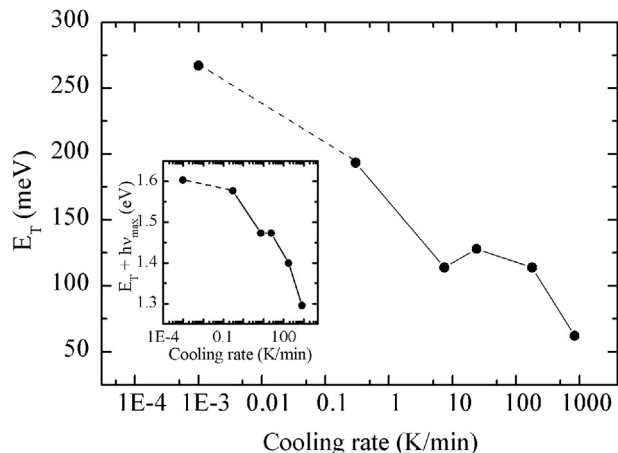


Fig. 4. The E_T values in dependence of the cooling rate. The sum of thermal quenching activation energy E_T and PL band peak position $h\nu_{\max}$ in dependence of the cooling rate are presented on the inset graph.

cooling rates above 7.5 K/min. The overall shift of the PL band towards lower energies with increasing cooling rate can be explained by the change in the bandgap energy due to the increasing concentration of defect clusters and resulting higher degree of disorder. Change from ordered to disordered CZTS induces additional shift in the bandgap energy, being smaller of about 0.1 eV for the disordered CZTS.

4. Conclusion

We can conclude that by changing the cooling rate, the nature of defects can be changed. In case of extensive cation sublattice disorder, the concentration of defect clusters is relatively high and radiative recombination involving defect clusters that induce local band gap decrease dominates at $T = 10$ K. Giving more time for establishing order in the crystal lattice at temperatures below the order-to-disorder transition temperature at 533 K, the concentration of defect clusters can be reduced. As a result, radiative recombination involving deep acceptor defect with ionization energy of about 200 meV is dominating in the PL spectra of CZTS polycrystals. Unfortunately, both of the observed recombination channels are detrimental to the solar cell performance, leading to lower open circuit voltages and reduced photocurrent.

Acknowledgements

This work was supported by the Estonian Science Foundation grants ETF 9369 and ETF 9346, by the institutional research funding IUT 19-28 of the Estonian Ministry of Education and Research, Estonian Centre of Excellence in Research, Project TK117, and by Estonian Material Technology Programme, Project AR12128.

References

- [1] Wei Wang, Mark T. Winkler, Oki Gunawan, Tayfun Gokmen, Teodor K. Todorov, Yu Zhu, David B. Mitzi, Device characteristics of CZTSSe Thin-Film Solar Cells With 12.6% Efficiency, *Adv. Energy Mater.*, <http://dx.doi.org/10.1002/aenm.201301465>.
- [2] <http://www.solar-frontier.com/eng/news/2014/C031367.html>.
- [3] Shiyong Chen, X.G. Gong, A. Walsh, S.H. Wei, Crystal and electronic band structure of $\text{Cu}_2\text{ZnSnX}_4$ ($X = \text{S}$ and Se) photovoltaic absorbers: first-principles insights, *Appl. Phys. Lett.* 94 (2009) 041903.
- [4] D. Huang, C. Persson, Band gap change induced by defect complexes in $\text{Cu}_2\text{ZnSnS}_4$, *Thin Solid Films* 535 (2013) 265–269.
- [5] S. Schorr, H.J. Hoebler, M. Tovar, A neutron diffraction study of the stannite-kesterite solid solution series, *Eur. J. Mineral.* 19 (2007) 65.

- [6] S. Schorr, The crystal structure of kesterite type compounds: a neutron and X-ray diffraction study, *Sol. Energy Mater. Sol. Cells* 95 (2011) 1482–1488.
- [7] Jonathan J.S. Scragg, Leo Choubrac, Alain Lafond, Tove Ericson, Charlotte Platzer-Björkman, A low-temperature order-disorder transition in $\text{Cu}_2\text{ZnSnS}_4$ thin films, *Appl. Phys. Lett.* 104 (2014) 041911.
- [8] Wolfgang G. Zeier, Christophe P. Heinrich, Tristan Day, Chatr Panithipongwut, Gregor Kieslich, Gunther Brunklaus, G. Jeffrey Snyder, Wolfgang Tremel, Bond strength dependent superionic phase transformation in the solid solution series $\text{Cu}_2\text{ZnGeSe}_{4-x}\text{S}_x$, *J. Mater. Chem. A* 2 (2014) 1790–1794.
- [9] M. Grossberg, J. Krustok, J. Raudoja, T. Raadik, The role of structural properties on deep defect states in $\text{Cu}_2\text{ZnSnS}_4$ studied by photoluminescence spectroscopy, *Appl. Phys. Lett.* 101 (2012) 102102.
- [10] M. Grossberg, J. Krustok, J. Raudoja, K. Timmo, M. Altosaar, T. Raadik, Photoluminescence and Raman study of $\text{Cu}_2\text{ZnSn}(\text{Se}_x\text{S}_{1-x})_4$ monograins for photovoltaic applications, *Thin Solid Films* 519 (2011) 7403–7406.
- [11] M. Grossberg, T. Raadik, J. Raudoja, J. Krustok, Photoluminescence study of defect clusters in $\text{Cu}_2\text{ZnSnS}_4$ polycrystals, *Curr. Appl. Phys.* 14 (3) (2014) 447–450.
- [12] Kunihiko Tanaka, Tomokazu Shinji, Hisao Uchiki, Photoluminescence from $\text{Cu}_2\text{ZnSnS}_4$ thin films with different compositions fabricated by a sputtering-sulfurization method, *Sol. Energy Mater. Sol. Cells* 126 (2014) 143–148.
- [13] J.P. Leitaó, N.M. Santos, P.A. Fernandes, P.M.P. Salomé, A.F. da Cunha, J.C. Gonzalez, G.M. Ribeiro, F.M. Matinaga, Photoluminescence and electrical study of fluctuating potentials in $\text{Cu}_2\text{ZnSnS}_4$ -based thin films, *Phys. Rev. B* 84 (2011) 024120.
- [14] M. Grossberg, P. Salu, J. Raudoja, J. Krustok, Micro-photoluminescence study of $\text{Cu}_2\text{ZnSnS}_4$ polycrystals, *J. Photonics for Energy* 3 (1) (2013) 030599.
- [15] A.P. Levanyuk, V.V. Osipov, Edge luminescence of direct-gap semiconductors, *Sov. Phys. Usp.* 24 (1981) 187–215.
- [16] J. Krustok, H. Collan, M. Yakushev, K. Hjelt, The role of spatial potential fluctuations in the shape of the PL bands of multinary semiconductor compounds, *Phys. Scr. T* 79 (1999) 179–182.
- [17] J. Krustok, H. Collan, K. Hjelt, Does the low temperature Arrhenius plot of the photoluminescence intensity in CdTe point towards an erroneous activation energy, *J. Appl. Phys.* 81 (1997) 1442–1445.